FEMS Microbiology Letters, 363, 2016, fnw104

doi: 10.1093/femsle/fnw104
Advance Access Publication Date: 18 April 2016
Research Letter

RESEARCH LETTER – Pathogens & Pathogenicity

The ferrichrome receptor A as a new target for *Pseudomonas aeruginosa* virulence attenuation

Keehoon Lee[1,2], Kang-Mu Lee[1], Junhyeok Go[1,2], Jae-Chan Ryu[2,3], Ji-Hwan Ryu[2,3] and Sang Sun Yoon[1,2,4,*]

[1]Department of Microbiology and Immunology, Yonsei University College of Medicine, Seoul, 120-752, Korea, [2]Brain Korea 21 PLUS Project for Medical Sciences, Yonsei University College of Medicine, Seoul, 120-752, Korea, [3]The Research Center for Human Natural Defense System, Yonsei University College of Medicine, Seoul, 120-752, Korea and [4]Institute for Immunology and Immunological Diseases, Yonsei University College of Medicine, Seoul, 120-752, Korea

*Corresponding author: Department of Microbiology and Immunology, Yonsei University College of Medicine, 134 Shinchon-dong, Seodaemun-gu, Seoul, 120-752, Korea. Tel: +82-2-2228-1824; Fax: +82-2-392-7088; E-mail: sangsun_yoon@yuhs.ac

One sentence summary: Antibiotics stimulate biofilm formation in *P. aeruginosa* for reasons to be further explored. A mutant of ferrichrome receptor A was defective in antibiotic-inducible biofilm formation and exhibited concomitant virulence attenuation.

Editor: Klaus Hantke

ABSTRACT

Pseudomonas aeruginosa is an opportunistic pathogen, known to develop robust biofilms. Its biofilm development increases when antibiotics are presented at subminimal inhibitory concentrations (MICs) for reasons that remain unclear. In order to identify genes that affect biofilm development under such a sublethal antibiotic stress condition, we screened a transposon (Tn) mutant library of PAO1, a prototype *P. aeruginosa* strain. Among ~5000 mutants, a *fiuA* gene mutant was verified to form very defective biofilms in the presence of sub-MIC carbenicillin. The *fiuA* gene encodes ferrichrome receptor A, involved in the iron acquisition process. Of note, biofilm formation was not decreased in the Δ*pch*Δ*pvd* mutant defective in the production of pyochelin and pyoverdine, two well-characterized *P. aeruginosa* siderophore molecules. Moreover, Δ*fiuA*, a non-polar *fiuA* deletion mutant, produced a significantly decreased level of elastase, a major virulence determinant. Mouse airway infection experiments revealed that the mutant expressed significantly less pathogenicity. Our results suggest that the *fiuA* gene has pleiotropic functions that affect *P. aeruginosa* biofilm development and virulence. The targeting of FiuA could enable the attenuation of *P. aeruginosa* virulence and may be suitable for the development of a drug that specifically controls the virulence of this important pathogen.

Keywords: *Pseudomonas aeruginosa*; virulence; ferrichrome receptor A

INTRODUCTION

Pseudomomas aeruginosa is the most common opportunistic human pathogen. It produces various virulence factors, including flagella, type IV pili, alkaline protease, elastase, lipopolysaccharide, phospholipase, exotoxin A, pyoverdine and pyochelin (Llamas *et al.* 2006). The expression of these various virulence determinants is regulated by complex signal transduction systems in response to changes in the surrounding environment.

A biofilm is defined as a community of microbes that attaches to certain surfaces and is normally covered with self-produced extracellular materials (ECMs). Biofilm infections present high

Received: 23 February 2016; **Accepted:** 14 April 2016

Table 1. Bacterial strains, plasmids and primers used in this study.

Strains, plasmids and primers	Description	Source
Bacterial strains		
E. coli SM10/λpir	*Donor strain, Kmr, thi-1, thr, leu, tonA, lacY, supE, recA::RP4-2-Tc::Mu, kpir*	Lab collection
PAO1	Prototype *P. aeruginosa* laboratory strain	Lab collection
Δ*fiuA*	PA01 with in-frame deletion of *PA0470* gene	This study
Δ*pch*Δ*pvd*	Pyochelin and pyoverdine synthesis-defective PAO1 mutant	Lab collection
Plasmids		
pCVD442	sacB suicide vector generated from pUM24	Lab collection
pBTK30	Transposon vector for the construction of a random mutant library, Gm^r	(Kim *et al.* 2012)
pJN105c	pJN105 with the gentamicin resistance marker replaced by a carbenicillin resistance marker	(Min *et al.* 2014)
Primers		
fiuA upstream (forward)	5′-AAAGAGCTCTACTGGGCGCTGGACATCA-3′	
fiuA upstream (reverse)	5′-TTCCCGCACCGTTTCTCCAAGCTACAAGTGGTGAGCGACG-3′	
fiuA downstream (forward)	5′- CGTCGCTCACCACTTGTAGCTTGGAGAAACGGTGCGGGAA-3′	
fiuA downstream (reverse)	5′-AAAGAGCTCTCAAGGAA GGCCAGCAGGT-3′	

resistance not only to antibiotics, but also to the host immune response (Laarman *et al.* 2012; Gellatly and Hancock 2013; Rieber *et al.* 2013). In addition, biofilms of microbial pathogens are a major cause of chronic infection, and ∼80% of all microbial infections are thought to be biofilm associated (Costerton, Stewart and Greenberg 1999). Remarkably, microbes growing in biofilms can be ∼1000 times more resistant to antibiotics than their planktonic counterparts (Hoiby *et al.* 2010). To achieve this high level of antibiotic resistance, biofilm-dwelling microbes use several biofilm-specific mechanisms, such as physical ECM barriers, persister cell formation and the starvation-induced stress response (Hoiby *et al.* 2010; Mulcahy *et al.* 2010; Nguyen *et al.* 2011; Sievert *et al.* 2013). Additional antibiotic resistance mechanisms of biofilms include glucan production and efflux pumps. Ethanol oxidation, extracellular DNA and iron acquisition are also thought to contribute to antibiotic resistance via as yet uncharacterized mechanisms (Zhang and Mah 2008; Hoiby *et al.* 2010; Sadovskaya *et al.* 2010; Mah 2012; Chen, Yu and Sun 2013). The siderophores pyoverdine and pyochelin are known to play particularly important roles in the evasion of the host immune response and biofilm development (Shen *et al.* 2005; Nadal Jimenez *et al.* 2010; Peek *et al.* 2012). The iron uptake system of *P. aeruginosa*, which involves pyoverdin and pyochelin, has been highly studied. However, information regarding the ferrichrome uptake system in *P. aeruginosa* is very limited. Ferrichrome is a heterologous hydroxamate siderophore that is involved in iron acquisition along with pyoverdine and pyochelin in *P. aeruginosa*. Approximately 80% of all ferrichrome is transferred into the cytoplasm through ferrichrome receptor protein A (FiuA) (Hannauer *et al.* 2010). As for ferripyoverdine and ferripyochelin, energy is required for ferrichrome to be transferred into the cytoplasm. This energy is supplied by an inner membrane protein, TonB1 (Hoegy *et al.* 2005; Llamas *et al.* 2006; Hannauer *et al.* 2010). TonB1 has been shown to be associated with quorum sensing, which is closely linked to biofilm formation (Abbas *et al.* 2007). Previous studies have also identified a link between biofilm formation and iron acquisition (Nadal Jimenez *et al.* 2010; Smith *et al.* 2013; Oglesby-Sherrouse *et al.* 2014).

Previous studies have shown that biofilm development by *P. aeruginosa* is enhanced in the presence of subminimal inhibitory concentration (sub-MIC) treatments of several antibiotics (Hoffman *et al.* 2005; Wang *et al.* 2010; Kaplan 2011). However, the genetic basis underlying this phenomenon has not yet been discovered. In this study, we screened a *P. aeruginosa* transposon mutant library to identify mutants that form defective biofilms in the presence of sub-MIC carbenicillin. We found that a *P. aeruginosa* mutant defective in the ferrichrome receptor A gene (*fiuA*) exhibited a dramatic decrease in biofilm formation under sub-MIC carbenicillin but not under non-antibiotic treated conditions. Importantly, other indications of virulence were also noticeably decreased when the *fiuA* gene was disrupted. This information will potentially be useful in the development of novel therapeutics against *P. aeruginosa* infection.

MATERIALS AND METHODS

Bacterial strains, plasmids, media and culture conditions

All bacterial strains and plasmids used in this study are listed in Table 1. Bacterial cultures were grown at 37°C in Luria–Bertani (LB) medium (10 g of tryptone, 5 g of yeast extract and 10 g of NaCl per liter). To screen for biofilm-defective mutants at sub-MICs, transposon-inserted bacterial strains were grown in 96-well plates containing 100 μl of LB with 9 μg/ml carbenicillin.

Construction of the *fiuA* deletion mutant

The *fiuA* deletion mutant was created by allelic replacement as previously described (Lee *et al.* 2012). Briefly, flanking sequences (∼500 bp) at both ends of the *fiuA* gene locus were PCR amplified with primers listed in Table 1. The SacI restriction sites are designated by underlining (Table 1). Two inner primers (upstream reverse primer and downstream forward primer) are complementary to each other. In this strategy, the 3′ end of the upstream sequence and the 5′ end of the downstream sequence are able to anneal during PCR amplification without further treatment. The deletion of the *fiuA* gene was confirmed by PCR, and the resultant strain was designated as Δ*fiuA*.

Iron acquisition capability assay

The PAO1, Δ*fiuA* and Δ*pch*Δ*pvd* mutants were incubated in LB medium at 37°C for 24 h. Siderophore activities in bacterial supernatants were quantified using a SideroTec Kit (Emergenbio, Ireland), an assay kit that detects siderophore in a sample

by color change. The assay kit is based on the chrome azurol sulfonate (CAS) assay which was developed by Schwyn and Neilands (1987). The blue reagent turns to purple or pink when ferric ion is transferred to siderophore, present in a sample.

Biofilm growth and quantification

Biofilms were prepared as previously described (O'Toole 2011). Briefly, a static biofilm was prepared by inoculating LB-grown bacterial strains (1:100 dilution) in LB or LB with carbenicillin in 96-well plates (SPL, Korea). The 96-well biofilm plates were incubated at 37°C for 24 h. Biofilm formation was quantified via the crystal violet (CV) assay, described by O'Toole (O'Toole 2011). The eluted CV stain was diluted (1:5) into a new 96-well plate and the absorbance of each well was read at 550 nm (O'Toole 2011).

Confocal laser scanning microscopy (CLSM) image analysis of biofilms

Differential interference contrast (DIC) images were acquired using a confocal laser scanning microscope (FV-1000; Olympus Optical Co. Ltd, Japan) equipped with FV10-ASW operating software (ver. 02.01). For CLSM image analysis, biofilms were prepared in 96-well optical bottom plates with a coverglass base (Nunc, MicroWell). After 24 h of biofilm growth, the planktonic portions of the cultures were discarded and the wells were washed with 0.9% saline. Alternatively, biofilms were grown in coverglass bottom dishes (SPL, Korea) in the same manner as in the 96-well plates. Biofilms were stained with a LIVE/DEAD BacLight Bacterial Viability kit (Invitrogen) and examined with two different wavelength lasers, 488 nm and 594 nm. For three-dimensional (3D) image analysis, Z-stack images were obtained and 3D images were reconstructed using FV10-ASW software.

Random transposon mutagenesis

For random transposon insertion mutagenesis, PAO1 was conjugated with *Escherichia coli* SM10/λpir cells harboring the pBTK30 plasmid (Table 1) (Kim *et al*. 2012). Gentamicin-resistant transconjugants were grown on LB agar plates containing 50 μg/ml gentamicin and 50 μg/ml Irgasan (Sigma). Approximately 5000 mutants were screened. All mutants defective in biofilm development under sub-MIC carbenicillin treatments were selected and their transposon insertion sites were determined by arbitrary PCR (Kim *et al*. 2012).

Elastase assay and *Caenorhabditis elegans* survival assay

The level of elastase activity in bacterial culture supernatants was assessed following procedures described elsewhere (Senturk *et al*. 2012; Gi *et al*. 2014). The levels of elastase in the whole-cell lysates and bacterial supernatants were assessed by probing membranes with anti-rabbit elastase antibody as a primary antibody (Lee *et al*. 2011). A *P. aeruginosa* virulence assay using *C. elegans* as an infection host was performed as described previously (Go *et al*. 2014). Briefly, overnight cultures of each bacterial strain were diluted 100-fold into LB broth and cultured until the OD_{600} value reached ∼1.0. Next, 10 μl of *E. coli* OP50 (negative control strain), PAO1 and Δ*fiuA* suspensions were spotted onto Nematode Growth Media (NGM) agar plates. After 2 h incubation at room temperature, each plate was seeded with 10 L4-stage hermaphrodite worms (three replicates per trial). Plates were incubated at 20°C. Live worms were transferred to a new NGM plate and scored for mortality every 24 h.

Murine airway infection model for *in vivo* virulence experiments

All animal experiments were approved by the Committee on the Ethics of Animal Experiments of Yonsei University College of Medicine (IACUC permit number: 2013-0369-5). To test the virulence of the Δ*fiuA* strain *in vivo*, 8-week-old C57BL/6N inbred female mice (Orient, Korea) were infected with each bacterial strain according to the acute infection protocol (Filloux and Ramos 2014). Infections were conducted through the intranasal route by making each mouse inhale 50 μl of the appropriate bacterial culture dilution, applied in a dropwise manner on the nose. Infected mice were returned to the cage and monitored for labored respiration, loss of ability to ambulate and survival in every 4 h until 24 h, then euthanized by cervical dislocation after anesthetization for histological observation of the lungs at the humane endpoint. For histological staining, lungs were perfused with sterile phosphate-buffered saline (PBS), and hematoxylin and eosin (H&E) staining was performed according to a standard protocol (Filloux and Ramos 2014). For the bacterial burden measurement, another set of mice ($n = 5$) were intranasally infected with 5×10^6 cells of PAO1 or Δ*fiuA*, using the same method as above. The lungs and spleens from the infected mice were collected at 16 h after the infection. The harvested left lobes of lungs and spleens were homogenized, and the numbers of bacteria in the organ were measured by viable cell count assay.

Statistical analysis

All data are expressed as means ± standard deviation (SD). The unpaired Student's *t*-test and one-way analysis of variance (ANOVA) were used to analyze the significance of all comparisons. *P*-values <0.05 were considered to indicate statistical significance. All experiments were repeated at least three times for reproducibility.

RESULTS

Identification of a mutant defective in biofilm development under sub-MIC carbenicillin

The screen for mutants defective in biofilm development under sub-MIC antibiotic treatment conditions was conducted with 5000 transposon insertion mutants. All mutants that exhibited growth defects were first eliminated from the screening. Next, CV assays were performed for all mutants in 96-well plates, and all biofilm-defective mutants were identified. All selected mutants were validated in the second round of the CV assays. The transposon insertion site of each selected mutant was determined by arbitrary PCR, followed by DNA sequencing (data not shown). Twelve transposon-inserted mutants were left after the growth and biofilm formation screening steps. Six out of the 12 mutants that showed defective biofilm formation under sub-MIC conditions have a transposon insertion in the genes known to affect biofilm formation, such as *pelA*, *pelD*, *flgK* and *gacA* (data not shown). Finally, the transposon mutant PATN715 was selected. The ability of PATN715 to form biofilms was confirmed in normal and sub-MIC carbenicillin treatment conditions using the CV assay (Fig. 1A) and CLSM image analysis (Fig. 1B). The PAO1 and PATN715 strains displayed similar levels of biofilm formation in LB medium. However, the PAO1 biofilm was increased under sub-MIC carbenicillin treatment, whereas the PATN715 biofilm was decreased in this condition (Fig. 1A). Both CV

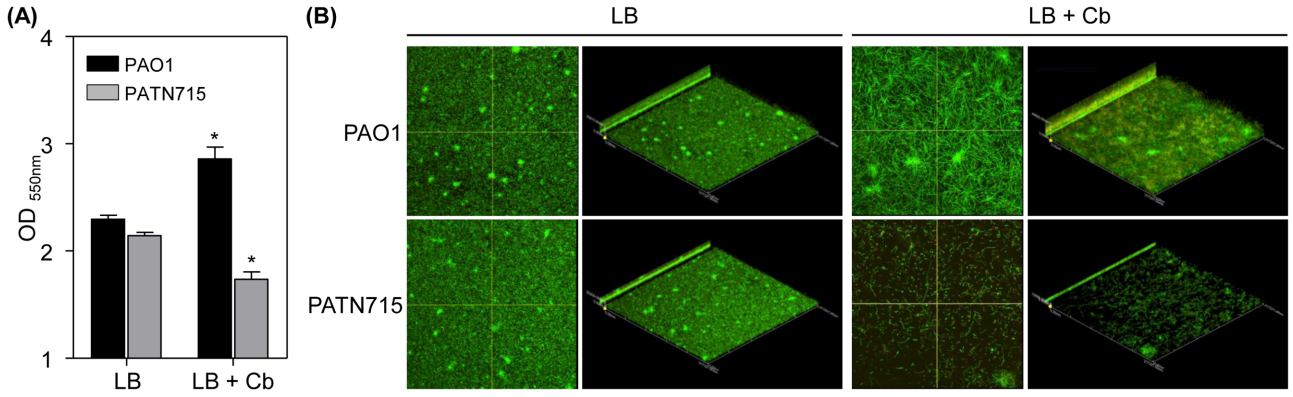

Figure 1. Identification of a mutant defective in biofilm development under sub-MIC carbenicillin treatment. (**A**) Crystal violet biofilm assay of PAO1 (black bars) and PATN715 (gray bars) strains grown in LB or LB with 9 μg/ml carbenicillin for 24 h. Six replicates were performed; values are expressed as means ± SDs. $^{*}P < 0.001$ vs. each biofilm grown in LB. (**B**) Transverse confocal scanning laser microscopy (CSLM) images and three-dimensional CSLM images of static biofilms of PAO1 and PATN715 bacteria grown in LB or LB with 9 μg/ml carbenicillin (x400). Biofilms were grown for 24 h.

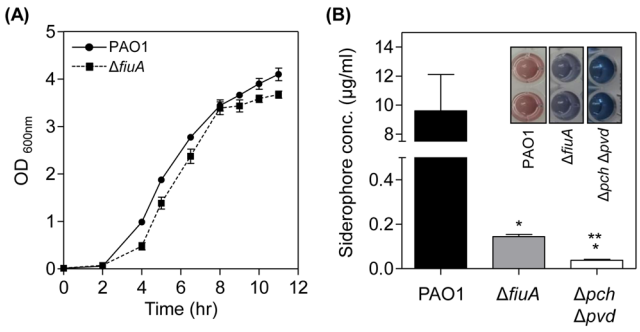

Figure 2. *fiuA* deletion effect for growth and siderophore activity of *P. aeruginosa*. (**A**) Growth rates of the PAO1 (solid line) and *fiuA* deletion mutant (Δ*fiuA*, dotted line) strains. Growth was measured by taking the optical density at 600 nm ($OD_{600\ nm}$). Three replicates were performed; data are expressed as the mean ± SD. (**B**) Siderophore assay of PAO1, Δ*fiuA* and the Δ*pch*Δ*pvd* double mutant. The color of the indicator reagent changes from blue to pink when siderophores exist in the samples. The number of replicates was three, and values of the mean ± SD are displayed in each bar. $^{*}P < 0.001$ vs. siderophore concentration of PAO1. $^{**}P < 0.05$ vs. siderophore concentration of the Δ*pch*Δ*pvd* double mutant.

assay and CLSM analysis presented consistent results. In addition, CLSM image analysis showed bacterial cell elongation in both PAO1 and PATN715 biofilms under antibiotic treatment (Fig. 1B). The transposon was determined to be inserted at the *fiuA* gene based on our arbitrary PCR, and its insertion was further confirmed by PCR (data not shown). DNA sequencing revealed that the transposon was inserted at 2039 bp downstream from the 5′ end of the *fiuA* gene (data not shown).

Various virulence-associated phenotypes were affected in Δ*fiuA*, a *fiuA* clean deletion mutant

To better elucidate the effects of the *fiuA* gene on bacterial phenotypes, we constructed an in-frame deletion mutant of the *fiuA* gene. Bacterial growth was not affected by the Δ*fiuA* mutation (Fig. 2A). Both strains, PAO1 and its Δ*fiuA* mutant, entered the exponential phase ∼4 h after inoculation. The doubling times of the PAO1 and Δ*fiuA* strains during the exponential phase were ∼1.8 h and 2 h, respectively.

To determine the role of *fiuA* in the iron acquisition, the siderophore activity of PAO1 and Δ*fiuA* was measured. The qualitative indication for siderophore activity showed the color changes of PAO1 from blue to pink and Δ*fiuA* to purplish color, but there was no color change in the Δ*pch*Δ*pvd* sample since the pyochelin and pyoverdine are the major siderophores of *P. aeruginosa* (Fig. 2B). The quantitative measure of siderophore concentration presented a very low amount of siderophore in the Δ*fiuA* supernatant sample (Fig. 2B). The siderophore concentration of the PAO1 supernatant was ∼10 μg/ml, whereas the concentration of the Δ*fiuA* supernatant was ∼0.15 μg/ml, and the concentration of Δ*pch*Δ*pvd* was close to zero (Fig. 2B).

To determine precisely the role of *fiuA* in biofilm development, biofilm developments of different siderophore mutants in two different growth conditions, LB broth and LB broth with sub-MIC carbenicillin, were quantified by the CV assay (Fig. 3A). The Δ*fiuA* exhibited different patterns of biofilm formation in LB and LB with sub-MIC carbenicillin compared with the PAO1 and Δ*pch*Δ*pvd* strains. The PAO1 and Δ*pch*Δ*pvd* strains exhibited enhanced biofilm development in the presence of sub-MIC carbenicillin, whereas the biofilm development of the Δ*fiuA* strain was significantly decreased under the same conditions. CLSM image analysis of the biofilms yielded results consistent with those from the CV assay (Fig 3B). CLSM Z-stack images revealed that the PAO1 and Δ*pch*Δ*pvd* strains exhibited increased biofilm formation in the presence of sub-MIC carbenicillin, whereas Δ*fiuA* biofilm formation was significantly decreased under the same conditions. Moreover, the compositions of the PAO1 and Δ*fiuA* biofilms were different. Very few dead (red fluorescent) bacterial cells were detected in the Δ*fiuA* biofilm, whereas the PAO1 biofilm contained a considerable amount of dead bacterial cells in its matrix (Fig. 3B).

To determine whether the Δ*fiuA* strain exhibits any difference in virulence compared with the wild-type strain, the amounts of elastase in the culture supernatants were measured. Elastase is a major virulence factor produced by *P. aeruginosa* that can be detected by SDS–PAGE as a major band migrating at ∼33 kDa (Yoon *et al.* 2010). First, the Elastin Congo Red (ECR) assay revealed that the Δ*fiuA* supernatant contained a significantly lower level of elastase activity compared with the PAO1 and Δ*pch*Δ*pvd* supernatants (Fig. 4A). Western blot analysis revealed that the amounts of elastase in the whole-cell lysates from the different strains were not significantly different. However, the amount of elastase in the Δ*fiuA* supernatant was clearly decreased (Fig. 4B).

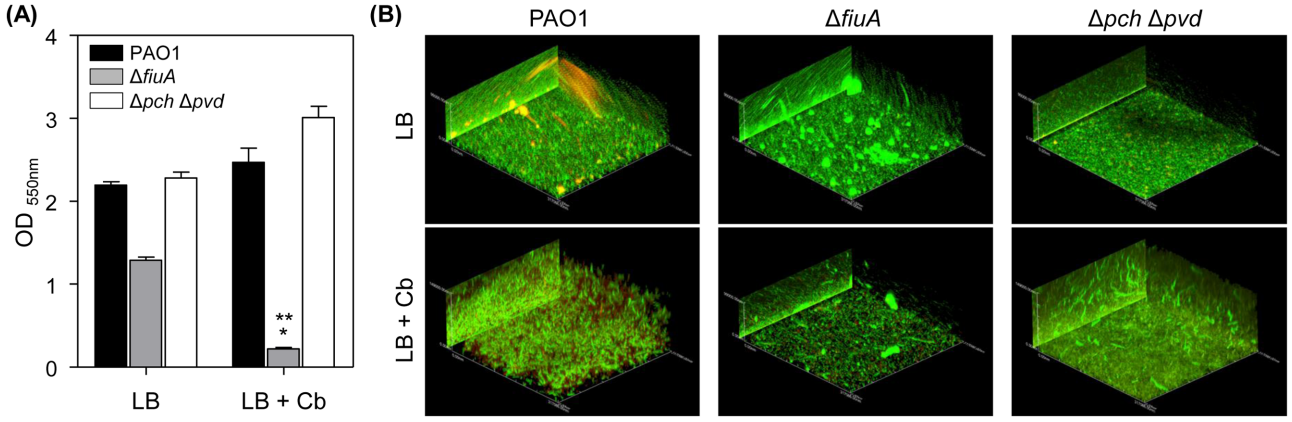

Figure 3. Biofilm development of various *P. aeruginosa* siderophore mutants under sub-MIC carbenicillin treatments. (**A**) Effects of sub-MIC carbenicillin treatments on biofilm development in PAO1 and siderophore mutant *P. aeruginosa* strains. Strains shown are PAO1 (black), Δ*fiuA* (gray) and Δ*pch*Δ*pvd* (white). Six replicates were performed; values are expressed as means ± SDs. *$P < 0.001$ vs. LB-grown biofilm. **$P < 0.001$ vs. biofilm levels of PAO1 and the Δ*pch*Δ*pvd* mutant in LB + 9 μg/ml carbenicillin. (**B**) Confocal laser scanning microscopy images of the biofilm development of the indicated *P. aeruginosa* strains with or without sub-MIC carbenicillin treatment. Bacteria were grown in LB (top) or LB + 9 μg/ml carbenicillin (bottom) for 24 h in a coverglass bottom dish (SPL, Korea). Magnification, ×400.

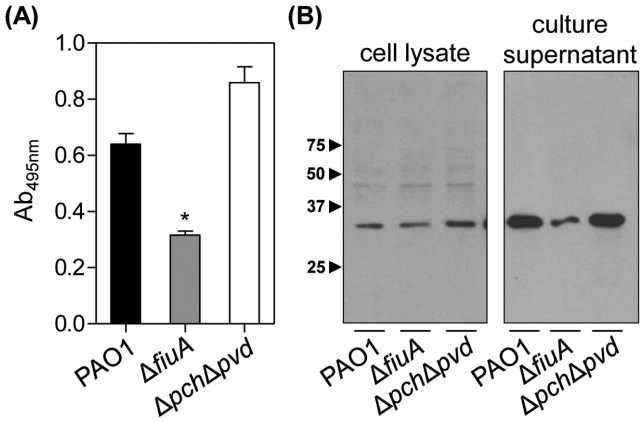

Figure 4. Decreased production of elastase by the *P. aeruginosa fiuA* deletion mutant. (**A**) Elastin Congo Red (ECR) assay of the elastase activities in the supernatants of PAO1 (black), Δ*fiuA* (gray) and Δ*pch*Δ*pvd* (white) cultures. Three replicates were performed; values are expressed as means ± SDs. (**B**) Western blot analysis of the elastase levels in the whole-cell lysates and supernatants of PAO1, Δ*fiuA* and Δ*pch*Δ*pvd* strains.

In vivo virulence of the Δ*fiuA* mutant was attenuated

We next sought to understand how the deletion of the *fiuA* gene affects the virulence of *P. aeruginosa in vivo*. For a preliminary study of *in vivo* virulence, *C. elegans* was used as a model for the multicellular eukaryotic organism. This experiment revealed that the Δ*fiuA*-fed *C. elegans* group has a higher survival rate compared with the PAO1-fed *C. elegans* group (Fig. 5A). The average life spans of the PAO1-fed and Δ*fiuA*-fed groups were 8.8 ± 0.8 and 12.1 ± 0.8 days, respectively, indicating that *C. elegans* grown on Δ*fiuA* bacteria possessed a 37.5% longer life span than those grown on PAO1 (Fig. 5A).

Likewise, mice ($n = 5$) infected with PAO1 or Δ*fiuA* cells (5.0×10^6 CFU) showed a contrasting survival rate. Two PAO1-infected mice perished at 22 h post-infection, whereas all Δ*fiuA*-infected mice survived up to 24 h (Fig. 5B). The survival assay was terminated at 24 h post-infection, at which time all surviving mice were euthanized for histological examination. H&E staining revealed more leukocyte infiltration in the lung tissues of PAO1-infected mice compared with those of Δ*fiuA*-infected mice (Fig. 5C). In addition to increased leukocyte infiltration, PAO1-infected mice also exhibited increased damage to the lung connective tissue (Fig. 5C). Furthermore, the bacterial counts in lungs of the mice revealed the definite difference in the infectivity of PAO1 and Δ*fiuA*. The average bacterial load in the lungs of PAO1-infected mice ($n = 5$) was 4.08×10^9 CFU per left lobe of lungs, whereas the average bacteria in the lungs of Δ*fiuA*-infected mice ($n = 5$) was 1.56×10^6 CFU per left lobe of lungs (Fig. 5D). The average bacterial load in the spleens of PAO1-infected mice ($n = 5$) was 1.14×10^7 CFU per spleen. Only one Δ*fiuA*-infected mouse presented a bacterial count of 3.33×10^4 CFU in its spleen, but bacterial cells were not recovered from the spleen of the other four Δ*fiuA*-infected mice (Fig. 5D).

DISCUSSION

A previous surveillance study revealed that antimicrobial usage and antimicrobial resistance are strongly correlated with each other (Xu *et al.* 2013). Bacterial resistance to antimicrobial agents is often mediated by the formation of biofilm, a protective mode of bacterial growth (Hoffman *et al.* 2005; Kaplan 2011). In this study, we sought to identify further genetic determinants that are responsible for antibiotic-inducible biofilm formation. After performing a forward genetic screen and subsequent validation processes, we identified the *fiuA* gene, deletion of which resulted in (i) defective biofilm formation under sublethal antibiotic stress; (ii) reduced elastase secretion; and (iii) decreased iron acquisition activity.

When PAO1 biofilm was treated with a subinhibitory concentration of imipenem, another β-lactam antibiotic, expression of genes encoding AmpC β-lactamase and proteins involved in alginate biosynthesis was increased (Bagge *et al.* 2004). Since alginate production occurs in the periplasmic space (Fata Moradali *et al.* 2015) and β-lactamases, in their mature forms, are also localized in the periplasm, it is highly likely that subinhibitory β-lactam treatment induces changes in the periplasmic environment. FiuA, as an outer membrane protein, interacts with FiuR that is an inner membrane-bound periplasmic protein (Hannauer *et al.* 2010). Therefore, these notions suggest that (i) functional FiuA protein may participate in bacterial responses to the subinhibitory β-lactam treatment by orchestrating the periplasmic reprogramming and (ii) the lack

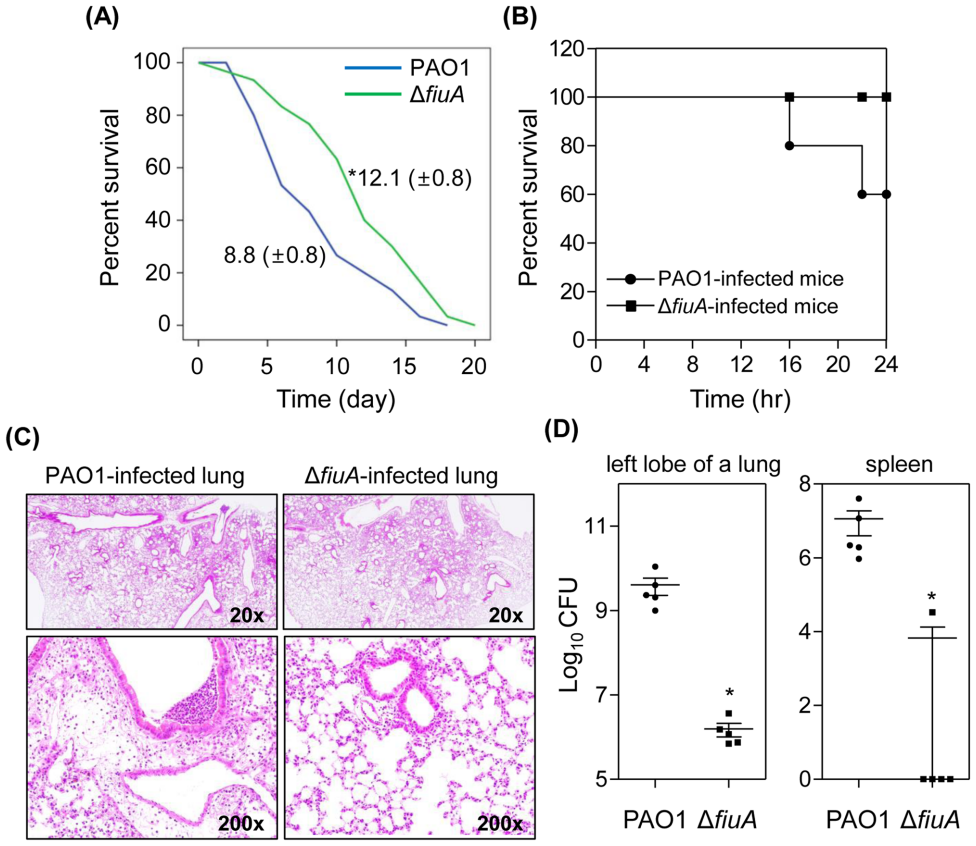

Figure 5. *In vivo* virulence analyses of the *fiuA* deletion mutant. (**A**) *C. elegans* survival curves of the PAO1-fed group (blue line) and the Δ*fiuA*-fed group (green line), and average life spans of each group of *C. elegans*. *$P < 0.01$ vs. the survival rate of the PAO1-fed worms. (**B**) Mouse survival rate following infection with PAO1 (circle) or the Δ*fiuA* mutant (square). (**C**) Histological analysis of H&E-stained lung tissues of intranasally infected mice with PAO1 are shown at ×20 and ×200 magnifications (infection dose: 5.0×10^6 CFU). (**D**) Bacterial counts recovered from the left lobes of lungs and spleens. The infection dose was 5.0×10^6 cells per mouse of PAO1 or Δ*fiuA*. *$P < 0.001$ vs. the CFU of the PAO1-infected mice.

of FiuA results in broader consequences that include defective biofilm formation and reduced elastase secretion. Consistent with this idea, the *arr* (aminoglycoside response regulator) gene, encoding a membrane-anchored enzyme, plays an essential role in aminoglycoside-inducible biofilm formation (Hoffman *et al.* 2005). Collectively, bacterial responses that end up with enhanced biofilm formation and altered virulence are probably accompanied by modifications of cell surface properties in *P. aeruginosa*.

Elastase is a major virulence factor of *P. aeruginosa* that is highly important for bacterial pathogenesis (Lee *et al.* 2011). ECR assays showed that pyochelin and pyoverdine production are not directly related to elastase production (Fig. 4A). Western blot analysis confirmed the ECR results obtained with the supernatants and also revealed that similar levels of elastase were present in between the cell lysates of PAO1 and the mutant strains (Fig. 4B). This result indicates that the production of elastase itself is not affected in the mutant strain, but the maturation of elastase may be affected by the deletion of the *fiuA* gene.

The average life span of *C. elegans* under normal growth conditions with *E. coli* OP50 bacteria is ~10.5 days (Go *et al.* 2014). We found that *C. elegans* fed on Δ*fiuA* bacteria displayed an even longer life span than *C. elegans* fed on *E. coli* OP50 (Fig. 5A). Moreover, the mice lung histology results confirm that the Δ*fiuA* strain has attenuated virulence, since the higher infiltration rate indicates that the bacterial strain is more virulent (Matute-Bello, Frevert and Martin 2008) (Fig. 5C). Four out of five Δ*fiuA*-infected mice did not present bacterial infections in the spleens (Fig. 5D). This indicates that the intranasal infection of Δ*fiuA* is unlikely to cause systemic infections.

Cumulatively, the data presented in this study reveal that the *fiuA* gene, encoding for *P. aeruginosa* ferrichrome receptor A (FiuA), has important functions in addition to its siderophore receptor function. Previous studies have proposed that *P. aeruginosa* virulence is related to iron acquisition, but most of these studies have focused on pyoverdine and pyochelin, or the ways in which iron transport mechanisms can contribute to antibiotic efflux systems (Cuiv *et al.* 2007; Mettrick and Lamont 2009; Imperi *et al.* 2010; Nadal Jimenez *et al.* 2010; Draper *et al.* 2011; Peek *et al.* 2012; Oglesby-Sherrouse *et al.* 2014). These do not identify the precise role of ferrichrome itself. We identified a direct relationship between FiuA and *P. aeruginosa* virulence. Specifically, we found that FiuA is involved in biofilm enhancement under sub-MIC antibiotic treatment and also in elastase production. However, the exact mechanisms underlying these results are still under investigation.

While the murine airway infection model is a good representation of acute *P. aeruginosa* infection, this model may not accurately represent chronic airway infections, which are the major form of infections in patients with cystic fibrosis (Ciofu *et al.* 2012). Further studies of the *fiuA* deletion effects in chronic infection models are necessary to understand fully FiuA involvement in *P. aeruginosa* virulence. Despite these limitations, our

results clearly demonstrate that FiuA is involved in the production of various *P. aeruginosa* virulence factors. In conclusion, this study identified new pleiotropic functions of *P. aeruginosa* FiuA in biofilm formation, elastase activity and *in vivo* infectivity. FiuA was found to be dispensable for *P. aeruginosa* growth. This is very important because the use of antibiotics that kill bacteria is known to induce the emergence of new antibiotic-resistant strains, which have the potential to threaten public health worldwide. Therefore, attenuating pathogen virulence instead of killing pathogens is an attractive strategy for novel therapeutics. By targeting FiuA, it may be possible to develop a drug that specifically controls the pathogen virulence.

ACKNOWLEDGEMENTS

This work was supported by grants from the National Research Foundation (NRF) of Korea, funded by the Korean Government (MSIP), 2014R1A2A2A01002861 and 2014R1A4A1008625.

Conflict of interest. None declared.

REFERENCES

Abbas A, Adams C, Scully N *et al.* A role for TonB1 in biofilm formation and quorum sensing in Pseudomonas aeruginosa. *FEMS Microbiol Lett* 2007;**274**:269–78.

Bagge N, Schuster M, Hentzer M *et al.* Pseudomonas aeruginosa biofilms exposed to imipenem exhibit changes in global gene expression and beta-lactamase and alginate production. *Antimicrob Agents Chemother* 2004;**48**:1175–87.

Chen M, Yu Q, Sun H. Novel strategies for the prevention and treatment of biofilm related infections. *Int J Mol Sci* 2013;**14**:18488–501.

Ciofu O, Mandsberg LF, Wang H *et al.* Phenotypes selected during chronic lung infection in cystic fibrosis patients: implications for the treatment of Pseudomonas aeruginosa biofilm infections. *FEMS Immunol Med Microbiol* 2012;**65**:215–25.

Costerton JW, Stewart PS, Greenberg EP. Bacterial biofilms: a common cause of persistent infections. *Science* 1999;**21**:1318–22.

Cuiv PO, Keogh D, Clarke P *et al.* FoxB of Pseudomonas aeruginosa functions in the utilization of the xenosiderophores ferrichrome, ferrioxamine B, and schizokinen: evidence for transport redundancy at the inner membrane. *J Bacteriol* 2007;**189**:284–7.

Draper RC, Martin LW, Beare PA *et al.* Differential proteolysis of sigma regulators controls cell-surface signalling in Pseudomonas aeruginosa. *Mol Microbiol* 2011;**82**:1444–53.

Fata Moradali M, Donati I, Sims IM *et al.* Alginate polymerization and modification are linked in Pseudomonas aeruginosa. *MBio* 2015;**6**:e00453–00415.

Filloux A, Ramos J-L (eds). *Pseudomonas methods and protocols*. NJ: Humana Press, 2014.

Gellatly SL, Hancock RE. Pseudomonas aeruginosa: new insights into pathogenesis and host defenses. *Pathog Dis* 2013;**67**:159–73.

Gi M, Jeong J, Lee K *et al.* A drug-repositioning screening identifies pentetic acid as a potential therapeutic agent for suppressing the elastase-mediated virulence of Pseudomonas aeruginosa. *Antimicrob Agents Chemother* 2014;**58**:7205–14.

Go J, Lee KM, Park Y *et al.* Extended longevity and robust early-stage development of Caenorhabditis elegans by a soil microbe, Lysinibacillus sphaericus. *Environ Microbiol Rep* 2014;**6**:730–7.

Hannauer M, Barda Y, Mislin GL *et al.* The ferrichrome uptake pathway in Pseudomonas aeruginosa involves an iron release mechanism with acylation of the siderophore and recycling of the modified desferrichrome. *J Bacteriol* 2010;**192**:1212–20.

Hoegy F, Celia H, Mislin GL *et al.* Binding of iron-free siderophore, a common feature of siderophore outer membrane transporters of Escherichia coli and Pseudomonas aeruginosa. *J Biol Chem* 2005;**280**:20222–30.

Hoffman LR, D'Argenio DA, MacCoss MJ *et al.* Aminoglycoside antibiotics induce bacterial biofilm formation. *Nature* 2005;**436**:1171–5.

Hoiby N, Bjarnsholt T, Givskov M *et al.* Antibiotic resistance of bacterial biofilms. *Int J Antimicrob Agents* 2010;**35**:322–32.

Imperi F, Tiburzi F, Fimia GM *et al.* Transcriptional control of the pvdS iron starvation sigma factor gene by the master regulator of sulfur metabolism CysB in Pseudomonas aeruginosa. *Environ Microbiol* 2010;**12**:1630–42.

Kaplan JB. Antibiotic-induced biofilm formation. *Int J Artif Organs* 2011;**34**:737–51.

Kim S, Rahman M, Seol SY *et al.* Pseudomonas aeruginosa bacteriophage PA1O requires type IV pili for infection and shows broad bactericidal and biofilm removal activities. *Appl Environ Microbiol* 2012;**78**:6380–5.

Laarman AJ, Bardoel BW, Ruyken M *et al.* Pseudomonas aeruginosa alkaline protease blocks complement activation via the classical and lectin pathways. *J Immunol* 2012;**188**:386–93.

Lee KM, Park Y, Bari W *et al.* Activation of cholera toxin production by anaerobic respiration of trimethylamine N-oxide in Vibrio cholerae. *J Biol Chem* 2012;**287**:39742–52.

Lee KM, Yoon MY, Park Y *et al.* Anaerobiosis-induced loss of cytotoxicity is due to inactivation of quorum sensing in Pseudomonas aeruginosa. *Infect Immun* 2011;**79**:2792–800.

Llamas MA, Sparrius M, Kloet R *et al.* The heterologous siderophores ferrioxamine B and ferrichrome activate signaling pathways in Pseudomonas aeruginosa. *J Bacteriol* 2006;**188**:1882–91.

Mah TF. Regulating antibiotic tolerance within biofilm microcolonies. *J Bacteriol* 2012;**194**:4791–2.

Matute-Bello G, Frevert CW, Martin TR. Animal models of acute lung injury. *Am J Physiol Lung Cell Mol Physiol* 2008;**295**:L379–99.

Mettrick KA, Lamont IL. Different roles for anti-sigma factors in siderophore signalling pathways of Pseudomonas aeruginosa. *Mol Microbiol* 2009;**74**:1257–71.

Min KB, Lee KM, Oh YT *et al.* Nonmucoid conversion of mucoid Pseudomonas aeruginosa induced by sulfate-stimulated growth. *FEMS Microbiol Lett* 2014;**360**:157–66.

Mulcahy LR, Burns JL, Lory S *et al.* Emergence of Pseudomonas aeruginosa strains producing high levels of persister cells in patients with cystic fibrosis. *J Bacteriol* 2010;**192**:6191–9.

Nadal Jimenez P, Koch G, Papaioannou E *et al.* Role of PvdQ in Pseudomonas aeruginosa virulence under iron-limiting conditions. *Microbiology* 2010;**156**:49–59.

Nguyen D, Joshi-Datar A, Lepine F *et al.* Active starvation responses mediate antibiotic tolerance in biofilms and nutrient-limited bacteria. *Science* 2011;**334**:982–6.

Oglesby-Sherrouse AG, Djapgne L, Nguyen AT *et al.* The complex interplay of iron, biofilm formation, and mucoidy affecting antimicrobial resistance of Pseudomonas aeruginosa. *Pathog Dis* 2014;**70**:307–20.

O'Toole GA. Microtiter dish biofilm formation assay. *J Vis Exp* 2011;**47**:2437.

Peek ME, Bhatnagar A, McCarty NA *et al.* Pyoverdine, the major siderophore in Pseudomonas aeruginosa, evades NGAL recognition. *Interdiscip Perspect Infect Dis* 2012;**2012**:843509.

Rieber N, Brand A, Hector A *et al.* Flagellin induces myeloid-derived suppressor cells: implications for Pseudomonas aeruginosa infection in cystic fibrosis lung disease. *J Immunol* 2013;**190**:1276–84.

Sadovskaya I, Vinogradov E, Li J *et al.* High-level antibiotic resistance in Pseudomonas aeruginosa biofilm: the ndvB gene is involved in the production of highly glycerol-phosphorylated beta-(1→3)-glucans, which bind aminoglycosides. *Glycobiology* 2010;**20**:895–904.

Schwyn B, Neilands JB. Universal chemical assay for the detection and determination of siderophores. *Anal Biochem* 1987;**160**:47–56.

Senturk S, Ulusuy S, Bosgelmez-Tinaz G *et al.* Quorum sensing and virulence of Pseudomonas aeruginosa during urinary tract infections. *J Infect Dev Ctries* 2012;**6**:501–7.

Shen JS, Geoffroy V, Neshat S *et al.* FpvA-mediated ferric pyoverdine uptake in Pseudomonas aeruginosa: identification of aromatic residues in FpvA implicated in ferric pyoverdine binding and transport. *J Bacteriol* 2005;**187**:8511–5.

Sievert DM, Ricks P, Edwards JR *et al.* Antimicrobial-resistant pathogens associated with healthcare-associated infections: summary of data reported to the National Healthcare Safety Network at the Centers for Disease Control and Prevention, 2009–2010. *Infect Control Hosp Epidemiol* 2013;**34**:1–14.

Smith DJ, Lamont IL, Anderson GJ *et al.* Targeting iron uptake to control Pseudomonas aeruginosa infections in cystic fibrosis. *Eur Respir J* 2013;**42**:1723–36.

Wang Q, Sun FJ, Liu Y *et al.* Enhancement of biofilm formation by subinhibitory concentrations of macrolides in icaADBC-positive and -negative clinical isolates of Staphylococcus epidermidis. *Antimicrob Agents Chemother* 2010;**54**:2707–11.

Xu J, Duan X, Wu H *et al.* Surveillance and correlation of antimicrobial usage and resistance of Pseudomonas aeruginosa: a hospital population-based study. *PLoS One* 2013;**8**:e78604.

Yoon MY, Lee KM, Jeong SH *et al.* Heterogeneous virulence potential and high antibiotic resistance of Pseudomonas aeruginosa strains isolated from Korean pneumonia patients. *J Microbiol* 2010;**48**:518–25.

Zhang L, Mah TF. Involvement of a novel efflux system in biofilm-specific resistance to antibiotics. *J Bacteriol* 2008;**190**:4447–52.